



State-of-the-art electron beams for compact tools of ultrafast science

Peter Salén^{a,*}, Anatoliy Opanasenko^{a,b}, Giovanni Perosa^a, Vitaliy Goryashko^{a,c}

^a FREIA Laboratory, Department of Physics and Astronomy, Uppsala University, Ångströmlaboratoriet, 75120 Uppsala, Sweden

^b National Science Center 'Kharkiv Institute of Physics and Technology', Akademichna Str. 1, 61108 Kharkiv, Ukraine

^c RIKEN, SPring-8, 679-5148 Hyogo, Japan

ARTICLE INFO

Keywords:

Ultrafast electron diffraction
Inverse Compton scattering
Velocity bunching

ABSTRACT

We review state-of-the-art electron beams for single-shot megaelectronvolt ultrafast electron diffraction (MeV-UED) and compact light sources. Our primary focus is on sub-100 femtosecond electron bunches in the 2–30 MeV energy range. We demonstrate that our new and recent simulation results permit significantly improved bunch parameters for these applications.

1. Introduction

Electron beams with cutting-edge properties enable experiments of higher quality either using electron beams directly or via generation of bright X-rays. An important application of electron beams is ultrafast electron diffraction (UED) [1], which exploits short electron bunches of small emittance in the keV–MeV energy range to study the structural dynamics of matter. The moderate electron energy employed in UED, typically below 5 MeV, permits a compact laboratory-scale facility. The compactness is also a desirable property for powerful X-ray sources and can be achieved using inverse Compton scattering (ICS). The ICS sources thus offer a useful alternative to large-scale X-ray facilities such as synchrotron-radiation sources.

In this work, we investigate the state-of-the-art electron bunch properties in the 2–30 MeV range. Our main focus is on sub-100 femtosecond (fs) electron beams with sufficient charge for single-shot UED, or ICS applications, or as an injector for compact free-electron lasers (FELs) such as the proposed projects MariX (Italy) [2], CompactLight [3], and ultracompact FEL at UCLA [4]. Hence, we primarily target MeV beams since at relativistic speeds the transverse and longitudinal space-charge forces are suppressed. As part of the investigation we expand our recently published work [5] with new simulated electron bunch parameters appropriate for the above mentioned types of applications and place them into the context of the current status of the field.

2. Results and discussion

Fig. 1(a)–(d) depicts projections of the 4D distribution of electron bunch parameters relevant for MeV-UED and compact light sources, which are collected from recent design and experimental studies. The

subfigures present (a) rms emittance vs charge, (b) rms emittance vs rms duration, (c) rms duration vs charge, (d) relative rms energy spread vs rms duration. The parameters are also summarized in Table 1 along with additional complementary details. The majority of the results are achieved with photo guns and by means of shaping electron bunches in RF structures using velocity bunching methods [5–22], marked with squares, circles and pentagonal stars, or magnetic compressors [14, 23, 24], represented by triangles, and [22] by the black pentagonal star. The data points generated from our studies are highlighted using the pentagonal stars [5, 22]. Additionally, we denote with diamond symbols a few results based on laser plasma wakefield acceleration (LWFA) [25–27], and with asterisks results using optical fields for bunching [28, 29]. To distinguish beam energies below 5 MeV, which are more suitable for UED, we have left all symbols corresponding to beam energies above 5 MeV unfilled in Fig. 1. The blue dashed lines in Fig. 1 indicate the current frontiers of a specific parameter space. To surpass these frontiers, new approaches are necessary. The red and blue diamonds [25, 27] in Fig. 1(c) demonstrate that techniques such as LWFA are capable of providing extreme parameters well beyond the frontier. However, these points are excluded when defining the blue dashed lines due to the large energy spread, which is unsuitable for MeV-UED or ICS sources. The red dashed lines indicate the new frontier enabled by recent studies [5, 6] as described further below. The green fields in Fig. 1 show beam parameter regions suitable for sub-100 fs single-shot MeV-UED with borders estimated based on Ref. [1].

The definition of the frontiers depicted by the blue dashed lines in Fig. 1 is discussed in the following. In Fig. 1(a) two separate blue dashed lines are drawn for small and large charges Q . For $Q > 1$ pC the slope in the log–log plot is $1/3$ ($\epsilon_x \sim Q^{1/3}$), while for $Q < 1$ pC the corresponding slope is $1/4$ ($\epsilon_x \sim Q^{1/4}$). The slopes of these

* Corresponding author.

E-mail address: peter.salen@physics.uu.se (P. Salén).

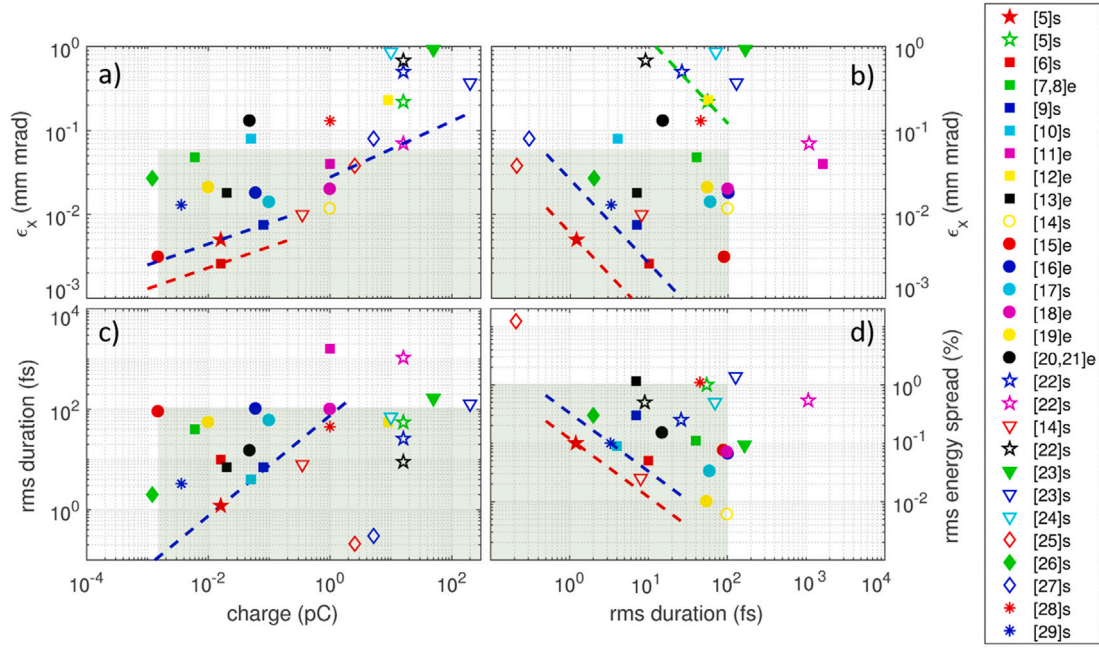


Fig. 1. Distributions of the state-of-the-art electron bunch parameters appropriate for MeV-UED and compact light sources (e.g. ICS sources). The unfilled symbols mark beam energies above 5 MeV. The letter ‘s’ or ‘e’ at the references indicates simulation or experimental results. The red and blue dashed lines represent the present state-of-the-art frontier (blue dashed line) and the new frontier predicted in our simulations [5] and those of Bartnik et al. [6] (red dashed line). The green dashed line in Fig. 1(b) provides an estimate of the slope for the blue dashed line, see further in the text. The green fields indicate beam parameter regions optimal for sub-100 fs single-shot MeV-UED.

Table 1

Summary of the state-of-the-art electron bunch parameters suitable for MeV-UED or compact light sources (e.g. ICS sources). E is electron bunch energy, Q is charge, σ_r is rms bunch duration, ϵ_x is transverse emittance, δE is relative rms energy spread and Size denotes the rms transverse electron-beam size. The letter s or e in the Ref. column indicates simulation or experimental results. In cases of different sizes or emittances in x and y direction the geometrical mean is given.

Ref.	E [MeV]	Q [pC]	σ_r [fs]	ϵ_x [nm]	δE [%]	Size [μm]
[5]s	3.3	0.016	1.2	5	0.1	240
[5]s	10	16	55	220	1	14
[6]s	4.5	0.016	10	2.6	0.05 ^a	5
[7,8]e	3	0.006	40	34 ^a		40 ^a
[9]s	5	0.08	7	7.5	0.3 ^a	560
[10]s	3.5	0.05	4	80	0.09	250
[11]e	3.5	1	1600	40		400
[12]e	5	9	56	230 ^a		95
[13]e	5	0.02	7	18	2.76 ^a	7.5
[14]s	7	1	100	11.7 ^a	0.006 ^a	100
[14]s	22.5	0.35	8	10	0.025	0.66
[15]e	4.2	0.0015	90	3.1	0.075	5
[16]e	3.7	0.06	102	18	0.066	86
[17]s	5	0.1	60	14	0.033	200
[18]e	3.1	1	100	20 ^a	0.07	250
[19]e	2.5	0.01	55	21 ^a	0.01	300
[20,21]e	3.4	0.048	15	130 ^a	0.15 ^a	170
[22]s	22.4	16	26	500	0.25	5
[22]s	21.1	16	1067	70	0.54	10
[22]s	26	16	9	680	0.5	3.8
[23]s	5	50	166	930	0.93	30
[23]s	22	200	128	370	1.38	32
[24]s	10	10	70	860	0.5 ^a	250
[25]s	5.8	2.55	0.21	38	12.3	0.065
[26]s	5	0.0012	2	27	0.3	170
[27]s	25	5.2	0.3	80		1.1
[28]s	2.1	1	45	130	1.1	35
[29]s	4.6	0.0036	3.3	13	0.1 ^a	1

^a Values were not given directly in the referenced study but have been estimated by us from other parameters.

lines are set according to the theoretical predictions, elaborated in the Appendix, assuming two limiting regimes of the photoemission from the cathode (1) space-charge limited emission (for high bunch charge), (2) photoemission-limited emission (for low bunch charge). The slope of the blue dashed line in Fig. 1(b) is estimated from the slope of the green dashed line, which intersects two data points (green and blue pentagonal stars) representing similar compression schemes and equal charge. The empirical dependence of the emittance on rms duration σ_r turned out to be $\epsilon_x \sim \sigma_r^{-1}$. With smaller charges such a line is expected to shift towards smaller emittance and bunch duration. One can observe that the blue dashed line approximately matches the frontier defined by data points from previous studies corresponding to the lower charge region, despite a slight variation in charge. In Fig. 1(c) the blue dashed line defines the frontier for electron bunches appropriate for MeV-UED. For such electron beams the thermal normalized emittance from the cathode is typically well conserved and therefore these data points can be distinguished from the rest. As one can see from Fig. 1(c) the empirical dependence of the rms duration on charge is $\sigma_r \sim Q$. The blue dashed line in Fig. 1(d) shows the present frontier with respect to the relative energy spread δE and rms bunch duration σ_r . For electron bunches of equal kinetic energy the frontier can be represented by a straight line with negative slope ($\delta E \sim \sigma_r^{-1}$) corresponding to a constant longitudinal phase space. Hence, the blue dashed line is drawn through the data points with similar kinetic energy and has a slope of -1 .

The red dashed lines represent the emergence of new frontiers enabled by the findings of Ref. [6], marked with the red filled square [see Fig. 1(a)], and our results [5], denoted with the red pentagonal star [Fig. 1(b),(d)]. It should be noted that our results represented by the red pentagonal star [5] and those by Bartnik et al. [6] were achieved using the same bunch charge of 16 fC, and by applying a similar approach to bunch shaping. This approach combines the half-wavelength velocity bunching, as first described in [5], with ballistic bunching. However, in Ref. [5] we performed simulations with the intrinsic emittance of the metallic photocathode corresponding to the theoretical mean transverse energy (MTE) of 86 meV [30], while the authors of Ref. [6] used MTE = 35 meV, assuming near threshold illumination of alkali antimonide photocathodes. The smaller MTE

reduced the emittance by a factor of two and enabled surpassing the frontier [see Fig. 1(a)]. By examination of Fig. 1 one observes that the red-filled square and red pentagonal star consistently lie inside the desired green region for single-shot MeV-UED applications and push the frontiers of the parameter space represented by the individual plots. It is also worth noting that the results associated with the red pentagonal star significantly advances single-shot UED into the sub-fs timescale region (with an rms bunch duration of 1.2 fs, and FWHM <0.3 fs [5]). We can conclude that a decreased MTE of photocathodes [6] and the use of half-wavelength velocity bunching combined with ballistic bunching [5,6] allows pushing the existing frontiers.

The green unfilled star indicates results using a similar compression scheme [5] but with a factor of 1000 times higher charge. These bunches are therefore better suited for ICS sources, which have reduced demands on emittance but require a relatively high charge compared to MeV-UED for maximizing photon flux. To provide new 16 pC bunch parameters, the simulations have also been expanded (blue, purple, and black unfilled stars). The half-wavelength velocity bunching [5] was applied to obtain the results denoted by the blue unfilled star, while the purple unfilled star corresponds to minimal emittance growth without applying any longitudinal compression. Fig. 1(a) shows that the purple unfilled star is located at the frontier with respect to bunch emittance and Fig. 1(c) reveals the competitive bunch duration associated with the blue unfilled star. The black unfilled star corresponds to the maximal longitudinal compression using magnetic-chicane compression optimized for ICS sources. Details of the chicane scheme can be found in Ref. [31]. The black unfilled star displays further reduction of the bunch duration for 16 pC charge [see Fig. 1(c)] and demonstrates that our chicane-compressed bunch opens the door to sub-10 fs X-ray pulses via ICS with almost two orders of magnitude higher charge than previously obtained with the emittance exchanger [14].

CRedit authorship contribution statement

Peter Salén: Writing – review & editing, Writing – original draft, Validation, Methodology, Investigation, Formal analysis. **Anatoliy Opanasenko:** Writing – review & editing, Writing – original draft, Visualization, Validation, Methodology, Investigation, Formal analysis. **Giovanni Perosa:** Writing – review & editing, Validation, Methodology, Formal analysis. **Vitaliy Goryashko:** Writing – review & editing, Validation, Supervision, Methodology, Formal analysis, Conceptualization.

Declaration of competing interest

The authors declare the following financial interests/personal relationships which may be considered as potential competing interests: Anatoliy Opanasenko reports financial support was provided by MSCA4Ukraine Consortium, funded by the European Union. Vitaliy Goryashko reports financial support was provided by Swedish Research Council. If there are other authors, they declare that they have no known competing financial interests or personal relationships that could have appeared to influence the work reported in this paper.

Acknowledgments

This work has received funding in part from Swedish Research Council (*Vetenskapsrådet*, 2022-03983) (acknowledged by VG), and through the MSCA4Ukraine project 1232628, which is funded by the European Union (acknowledged by AO). Views and opinions expressed are however those of the author only and do not necessarily reflect those of the European Union. Neither the European Union nor the MSCA4Ukraine Consortium as a whole nor any individual member institutions of the MSCA4Ukraine Consortium can be held responsible for them.

Appendix

The transverse emittance of an electron beam depends on the intrinsic (or thermal) emittance, the beam optics aberrations, space-charge-dominated emittance and emittance growth compensation methods [32–35]. The blue dashed lines in Fig. 1(a) represent a hard frontier, therefore they are determined by the initial intrinsic emittance assuming its conservation. In the log–log plot, the ideal hard frontier should correspond to a family of slopes depending on the limiting emission regime. Below, we exemplify two emission regimes: (1) space-charge limited emission (usually high bunch charge) and (2) photoemission-limited regime (often low bunch charge).

(I) Space-charge limited emission for short bunches

For short (pancake) bunches, the Child–Langmuir limit at the cathode reads

$$E_{acc} = \frac{Q}{\epsilon_0 \pi r_c^2}, \quad (1)$$

(where Q is the bunch charge, r_c is the beam radius, E_{acc} is the external electric field at the photocathode). The maximal charge of a short bunch can be obtained [36,37]

$$Q = I_A \frac{\sqrt{2}}{8} \left[\frac{e E_{acc} r_c}{m c^2} \right]^{\frac{2}{3}} \tau_{laser}, \quad (2)$$

where I_A is the Alphen's current, τ_{laser} is the laser pulse duration on the photocathode. Substituting (1) into (2) we can get

$$r_c = \left[I_A \frac{\sqrt{2}}{8} \tau_{laser} \right]^{\frac{2}{3}} \frac{e}{m c^2} \frac{Q^{\frac{1}{3}}}{\pi \epsilon_0}. \quad (3)$$

On the other hand, the thermal rms transverse normalized emittance of an emitted electron bunch is given by [38]

$$\epsilon_x = \frac{r_c}{2} \sqrt{\frac{MTE}{m c^2}}, \quad (4)$$

where MTE is the mean transverse energy. Substituting (3) into (4) we obtain

$$\epsilon_x = Q^{\frac{1}{3}} \frac{e}{2 \pi m c^2 \epsilon_0} \left[I_A \frac{\sqrt{2}}{8} \tau_{laser} \right]^{\frac{2}{3}} \sqrt{\frac{MTE}{m c^2}}. \quad (5)$$

(II) Laser pulse energy-limited emission

Consider again a short bunch but with a weak space-charge field such that

$$\frac{Q}{\epsilon_0 \pi r_c^2} \ll E_{acc}. \quad (6)$$

In this case, the bunch charge is defined by the energy of the laser pulse W_{laser} and the quantum efficiency of the photocathode QE

$$Q = e \frac{W_{laser}}{\hbar \omega} QE, \quad (7)$$

where the quantum efficiency is given by [38]

$$QE \approx \eta [MTE]^2. \quad (8)$$

Substituting (8) into (7) we obtain

$$Q^{\frac{1}{4}} = \left[e \frac{W_{laser}}{\hbar \omega} \eta \right]^{\frac{1}{4}} \sqrt{MTE}. \quad (9)$$

Taking into account (4) in the last Eq. (9), we can get the emittance as a function of charge in the case of laser pulse energy-limited emission

$$\epsilon_x = Q^{\frac{1}{4}} \frac{r_c}{2 \sqrt{m c^2}} \left[e \frac{W_{laser}}{\hbar \omega} \eta \right]^{-\frac{1}{4}}. \quad (10)$$

Data availability

Data will be made available on request.

References

- [1] D. Filippetto, et al., Ultrafast electron diffraction: Visualizing dynamic states of matter, *Rev. Modern Phys.* 94 (4) (2022) 104003.
- [2] MariX initiative, URL <https://marix.eu>.
- [3] CompactLightProject, URL <https://www.compactlight.eu>.
- [4] J.B. Rosenzweig, et al., An ultra-compact x-ray free-electron laser, *New J. Phys.* 22 (9) (2020) 093067.
- [5] A. Opanasenko, et al., Half-wavelength velocity bunching: non-adiabatic temporal focusing of charged particle beams, *New J. Phys.* 25 (12) (2023) 123049, <http://dx.doi.org/10.1088/1367-2630/ad1717>.
- [6] A. Bartnik, et al., Ultimate bunch length and emittance performance of an MeV ultrafast electron diffraction apparatus with a dc gun and a multicavity superconducting rf linac, *Phys. Rev. Accel. Beams* 25 (9) (2022) 093401.
- [7] M.A.K. Othman, et al., Measurement of femtosecond dynamics of ultrafast electron beams through terahertz compression and time-stamping, *Appl. Phys. Lett.* (ISSN: 1077-3118) 122 (14) (2023) <http://dx.doi.org/10.1063/5.0134733>.
- [8] M.A.K. Othman, et al., Improved temporal resolution in ultrafast electron diffraction measurements through THz compression and time-stamping, *Struct. Dyn.* (ISSN: 2329-7778) 11 (2) (2024) <http://dx.doi.org/10.1063/4.0000230>.
- [9] K. Floettmann, Generation of sub-fs electron beams at few-MeV energies, *Nucl. Instrum. Methods Phys. Res. A* 740 (2014) 34–38.
- [10] R.K. Li, et al., Imaging single electrons to enable the generation of ultrashort beams for single-shot femtosecond relativistic electron diffraction, *J. Appl. Phys.* 110 (7) (2011) 074512.
- [11] R.K. Li, et al., Nanometer emittance ultralow charge beams from rf photoinjectors, *Phys. Rev. Spec. Top. - Accel. Beams* 15 (9) (2012) 090702.
- [12] X.H. Lu, et al., Generation and measurement of velocity bunched ultrashort bunch of pc charge, *Phys. Rev. Spec. Top. - Accel. Beams* 18 (3) (2015) 032802.
- [13] J. Maxson, et al., Direct measurement of sub-10 fs relativistic electron beams with ultralow emittance, *Phys. Rev. Lett.* 118 (15) (2017) 154802.
- [14] E.A. Nanni, et al., Nanomodulated electron beams via electron diffraction and emittance exchange for coherent x-ray generation, *Phys. Rev. Accelerat. Beams* 21 (1) (2018) 014401, <http://dx.doi.org/10.1103/physrevaccelbeams.21.014401>.
- [15] X. Shen, et al., Femtosecond mega-electron-volt electron microdiffraction, *Ultramicroscopy* 184 (2018) 172–176.
- [16] S.P. Weathersby, et al., Mega-electron-volt ultrafast electron diffraction at SLAC national accelerator laboratory, *Rev. Sci. Instrum.* 86 (7) (2015) 073702.
- [17] J. Yang, et al., Femtosecond pulse radiolysis and femtosecond electron diffraction, *Nucl. Instrum. Methods Phys. Res. A* 637 (1) (2011) S24–S29.
- [18] J. Yang, Y. Yoshida, Relativistic ultrafast electron microscopy: Single-shot diffraction imaging with femtosecond electron pulses, *Adv. Condens. Matter Phys.* 2019 (2019) 1–6.
- [19] J. Yang, et al., A compact ultrafast electron diffractometer with relativistic femtosecond electron pulses, *Quantum Beam Sci.* 4 (1) (2020) 4.
- [20] L. Zhao, et al., Terahertz streaking of few-femtosecond relativistic electron beams, *Phys. Rev. X* 8 (2) (2018) 021061.
- [21] L. Zhao, et al., Terahertz oscilloscope for recording time information of ultrashort electron beams, *Phys. Rev. Lett.* 122 (14) (2019) 144801.
- [22] Parameters obtained in the present study.
- [23] A. He, et al., Design of low energy bunch compressors with space charge effects, *Phys. Rev. Spec. Top. - Accel. Beams* 18 (1) (2015) 014201.
- [24] K. Wang, et al., Longitudinal compression and transverse matching of electron bunch for external injection LPWA at ESCULAP, *Nucl. Instrum. Methods Phys. Res. A* 909 (2018) 266–270.
- [25] C. Bonțoiu, et al., TeV/m catapult acceleration of electrons in graphene layers, *Sci. Rep.* 13 (1) (2023) 1330.
- [26] J. Faure, et al., Concept of a laser-plasma-based electron source for sub-10-fs electron diffraction, *Phys. Rev. Accel. Beams* 19 (2) (2016) 021302.
- [27] P. Tomassini, et al., Attosecond pulses from ionization injection wakefield accelerators, *Instruments* 7 (4) (2023) 34.
- [28] A. Fallahi, et al., Short electron bunch generation using single-cycle ultrafast electron guns, *Phys. Rev. Accel. Beams* 19 (8) (2016) 081302.
- [29] C. Li, et al., Few-femtosecond MeV electron bunches for ultrafast electron diffraction, *Phys. Rev. Appl.* 17 (6) (2022) 064012.
- [30] G. Shamuilov, et al., Emittance self-compensation in blow-out mode, *New J. Phys.* 24 (12) (2022) 123008.
- [31] CDR Ångström laser, URL <https://indico.uu.se/event/1405/>.
- [32] B. Carlsten, New photoelectric injector design for the los alamos national laboratory XUV fel accelerator, *Nucl. Instrum. Methods Phys. Res. A* (ISSN: 0168-9002) 285 (1–2) (1989) 313–319, [http://dx.doi.org/10.1016/0168-9002\(89\)90472-5](http://dx.doi.org/10.1016/0168-9002(89)90472-5).
- [33] L. Serafini, J.B. Rosenzweig, Envelope analysis of intense relativistic quasilinear beams in rf photoinjectors: a theory of emittance compensation, *Phys. Rev. E* (ISSN: 1095-3787) 55 (6) (1997) 7565–7590, <http://dx.doi.org/10.1103/physreve.55.7565>, URL <http://dx.doi.org/10.1103/PhysRevE.55.7565>.
- [34] M. Ferrario, et al., Experimental demonstration of emittance compensation with velocity bunching, *Phys. Rev. Lett.* (ISSN: 1079-7114) 104 (5) (2010) <http://dx.doi.org/10.1103/physrevlett.104.054801>.
- [35] S. Di Mitri, et al., Scaling of beam collective effects with bunch charge in the CompactLight free-electron laser, *Photonics* 7 (4) (2020) 125.
- [36] D. Filippetto, et al., Maximum current density and beam brightness achievable by laser-driven electron sources, *Phys. Rev. Spec. Top. - Accel. Beams* 17 (2) (2014).
- [37] G. Shamuilov, et al., Child-Langmuir law for photoinjectors, *Appl. Phys. Lett.* 113 (20) (2018) 204103.
- [38] D.H. Dowell, J.F. Schmerge, Quantum efficiency and thermal emittance of metal photocathodes, *Phys. Rev. Spec. Top. - Accel. Beams* 12 (7) (2009).